The solid-to-liquid transition region of an Ag–Pd bimetallic nanocluster

The solid-to-liquid transition region of an Ag–Pd bimetallic nanocluster

D H Kim, H Y Kim, H G Kim, J H Ryu and H M Lee

Department of Materials Science and Engineering, Korea Advanced Institute of Science and
Technology, 335 Gwahangno (373-1, Guseong-dong), Yuseong-gu, Daejeon 305-701,
Republic of Korea

E-mail: hmlee@kaist.ac.kr

Abstract
The solid–liquid transition region of an Ag–Pd bimetallic cluster composed of 201 Ag and
201 Pd atoms is investigated by means of molecular dynamics simulation. An effective and
convenient method is reported for finding that region. For external energy, Ag and Pd clusters
were caused to collide with various initial velocities under the condition of a microcanonical
ensemble. The Ag201–Pd201 bimetallic cluster was observed to completely melt at 900 K with
a solid–liquid coexistence range of 50 K.

(Some figures in this article are in colour only in the electronic version)

1. Introduction

Nanosized materials have recently attracted considerable
attention due to their potential applications [1–5]. Numerous
studies have also focused on nanosized bimetallic clusters
because the properties of the clusters can be tuned in terms
of size and composition [6–8]. For the practical application
of bimetallic clusters, reasonable information on the solid-to-
liquid transition is necessary because it suggests a temperature
range in which the cluster can be used without structural
change.

Recently, information on the solid-to-liquid transition
region of nanoclusters has been obtained by molecular
simulation methods. Through detailed analyses with
caloric curves, the root mean square bond-length fluctuation,
heat capacity, and deformation parameters, the melting or
freezing points have been determined and reported [9, 10].
These computational works have been mostly carried out
under constant temperature conditions (NVT) and applied
specifically to unary clusters or clusters with magic
structures such as the icosahedron or truncated octahedron
structure [11–13].

Most molecular dynamics (MD) simulations on collision
or coalescence among clusters have also been performed under
constant temperature conditions (NVT) [14–16], which is
an ineffective method in terms of computation time. If the
constant energy condition (NVE) is used and the velocity
is given in collision simulations, then the kinetic energy is

externally added to the total energy of the system through
the velocity term. When the clusters collide each other, the
kinetic energy is suddenly decreased due to decreased velocity;
the potential energy is then decreased due to the decreased
surface areas. The excess energy gives rise to the temperature
increase. This annealing effect, which can shorten coalescence
times by enhancing atomic diffusion, is expected to induce the
structural evolution of the merged cluster and eventually induce
the melting. In this way, the solid-to-liquid transition behavior
and the range of the bimetallic cluster can be investigated.

In the present work, we suggest a convenient and effective
method of predicting the solid-to-liquid transition region of the
Ag–Pd bimetallic cluster by colliding two clusters of Ag and
Pd at a different velocity under a microcanonical ensemble
(NVE). This study, which is a continuation of our two
previous works [17, 18], is compared with the simulations on
collision or coalescence of nanosized free clusters [19–21].

It is well known that the melting of the surface
layer of clusters (surface melting) takes place before the
complete melting of nanoclusters. Surface melting has
been observed through density distribution functions, mean
square displacements, caloric curves, and configurations of
clusters [10, 14, 22, 23]. To date, however, there is still no clear
definition of surface melting. In this report, we set the surface
melting point as the temperature where the cluster atoms at
the surface start to disorder. The temperature also indicates
the premelting or lower temperature limit of the solid–liquid

Table 1. Parameters of the quantum Sutton–Chen potential for the Ag–Pd bimetallic nanocluster [24, 25] used in this study.

	n	m	ε (eV)	c	a (Å)
Ag–Ag	11	6	3.9450×10^{-3}	96.524	4.0691
Pd–Pd	12	6	3.2864×10^{-3}	148.205	3.8813

coexistence region in a complete solid-solution binary phase diagram.

2. Computational details

2.1. Quantum Sutton–Chen potential

We performed all our MD simulations by using the quantum Sutton–Chen many-body potentials [24, 25], an advanced form of the Sutton–Chen (SC) potential [26]. This approach includes quantum corrections and takes into account the zero-point energy (quantum) effect, thus allowing better prediction of temperature dependent properties. As such, it can be successfully applied to predict properties involving surface energies, vacancy energies, and stacking-fault energies, which cannot be precisely predicted with the SC potential.

Based on the SC-type potential, the total energy of the system can be predicted as follows:

$$U_{\text{tot}} = \sum_i U_i = \sum_i \varepsilon \left[\sum_{i \neq j} \tfrac{1}{2} V(r_{ij}) - c \rho_i^{1/2} \right] \qquad (1)$$

where r_{ij} is the distance between atoms i and j, c is a dimensionless parameter that scales the attractive terms, and ε sets the overall energy scale. Here, $V(r_{ij})$ is a pair potential that accounts for the repulsive force between atoms i and j, which result from the Pauli repulsion between core electrons:

$$V(r_{ij}) = \left(\frac{a}{r_{ij}} \right)^n. \qquad (2)$$

The contribution of the local electron density associated with an atom i is given by

$$\rho_i = \sum_{j \neq i} \phi(r_{ij}) = \sum_{j \neq i} \left(\frac{a}{r_{ij}} \right)^m. \qquad (3)$$

Here, $\phi(r_{ij})$ is a functional that specifies how the electron density of an atom depends on the distances from the neighboring atoms, a is a length parameter that scales all spacing (leading to the dimensionless V and $\phi(r_{ij})$), and n and m are integer parameters such that $n > m$. Table 1 shows all the potential parameters. We used combination rules to predict the interatomic potentials between different metal elements [25]. The geometric mean was used to obtain the energy scaling parameter, ε, and an arithmetic mean was used for n, m and a.

2.2. MD simulation details

Classical MD simulations were conducted. To solve Newton's dynamic equation, we applied a fifth-order Gear predictor–corrector algorithm [27] with a time step of 0.001 ps and, under

a condition of constant temperature, an NVT ensemble, the velocity rescaling was repeated after every MD time step.

Each cluster of Ag and Pd is composed of 201 atoms, which correspond to a face-centered cubic structure. Initially, we placed them in the center of a large simulation box (2000 Å × 2000 Å × 2000 Å). The two clusters were equilibrated for 200 ps at 200 K under an NVT ensemble with a separation distance of 30 Å between two clusters. Then, the equilibrated clusters were collided with certain values of initial moving velocity and additional 10^6 steps of MD runs (1 ns of production time) were performed under a condition of constant energy, an NVE ensemble. The same velocity, but with opposite signs, was applied to all the atoms of Pd and Ag clusters, respectively.

The initial velocity was varied from 100 to 700 m s^{-1} in increments of 50 m s^{-1}. The velocity increments were reduced (by 5 or 2 m s^{-1}) to acquire more detailed data near the solid-to-liquid transition region. The variation of the total energy and cluster temperature versus the MD simulation time was plotted and analyzed with corresponding cluster structures.

3. Results and discussion

When the initial velocity is below 440 m s^{-1} (350 m s^{-1} in figure 1(a) and 420 m s^{-1} in figure 1(b)), the final atomic configuration of the Ag–Pd cluster at 1 ns implies that it did not go through the liquid transition. At a velocity of 350 m s^{-1}, the two clusters were merged but, as seen in figure 1(a), the mixing in the atomic scale was not complete. Seemingly, the two clusters were in contact with each other. However, at 420 m s^{-1}, they were merged and mixed to form the typical core–shell structure shown in figure 1(b), which is the most stable structure of the Ag–Pd cluster system that has been reported [28]. More Ag atoms aggregated on the surface of the Pd cluster in the final morphology with an increase in the initial velocity in this velocity range. It is well known that Ag has a strong tendency to remain on the surface while Pd atoms are preferentially segregated in the center of the cluster because Ag has a lower surface energy than Pd [17, 18, 29, 30]. Therefore, it is likely that the kinetic energy supplied to this system through collision velocity was not high enough to enable the Ag–Pd cluster to go through the solid-to-liquid transition. All the energy must have been used in the surface diffusion of the Ag atoms.

After the released kinetic energy induced a rapid rise in temperature and structural evolution, the excess surface energy from the reduced total surface area provided an additional energy source and enabled the Ag–Pd bimetallic cluster to evolve continuously toward a more stable structure with a low potential energy state. The potential energy of the cluster is then gradually converted to kinetic energy, which scales the temperature. Thus, as seen in figures 2(a) and (b), the cluster temperature is increased. As more kinetic energy is supplied, the final temperature obviously becomes higher with an increase in the initial velocity.

When the initial velocity was higher than 440 m s^{-1} but below 496 m s^{-1}, (460 m s^{-1} in figure 1(c)), the final configuration showed a crystalline nature inside the cluster but
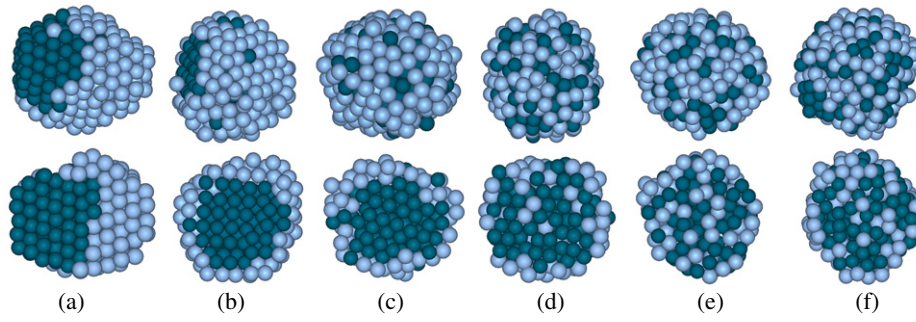
Figure 1. Final structure (top row) and cross section (bottom row) of the 201Ag–201Pd cluster after 1 ns of collision with different initial velocities: (a) 350 m s^{-1}; (b) 420 m s^{-1}; (c) 460 m s^{-1}; (d) 500 m s^{-1}; (e) 540 m s^{-1}; (f) 600 m s^{-1}. The Ag atoms are represented in light, the Pd atoms in dark.
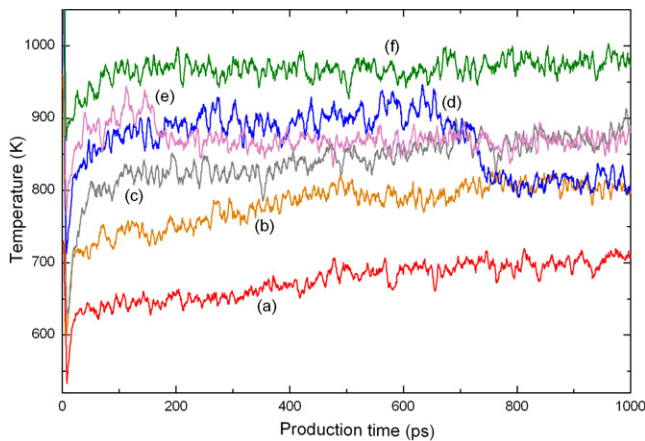
Figure 2. Evolution of temperature with time is shown at various initial velocities: (a) 350 m s^{-1}; (b) 420 m s^{-1}; (c) 460 m s^{-1}; (d) 500 m s^{-1}; (e) 540 m s^{-1}; (f) 600 m s^{-1}.

a noncrystalline nature at the surface. The surface melting most likely started in this velocity range. The cluster temperature is monotonically increased, as shown in figure 2(c), because the complete melting inside the cluster core has not yet occurred.

If the total amount of released kinetic energy in the collision exceeds a critical value, the cluster starts to undergo the solid-to-liquid transition, or melting, as demonstrated in figure 1(d) of 500 m s^{-1} and figure 1(e) of 540 m s^{-1}. This phenomenon corresponds to the velocity range of 496 to 560 m s^{-1}. Due to the liquid transition, as seen in figures 2(d) and (e), the temperature drops suddenly. The drop in temperature occurs because the potential energy of the liquid state is much higher than that of the solid state and, thus, the kinetic energy must be lowered in transition and, in turn, the temperature must be lowered. Figure 3(a) shows the sequential snapshot during MD simulation with 500 m s^{-1} of initial velocity. Right after collision, Ag atoms quickly diffused on the cluster surface (similar to figures 1(a) and (b)) and the Ag–Pd cluster changed to a core–shell structure followed by disordering of the surface layer (surface melting as in figure 1(c)) and finally the Ag–Pd cluster was entirely melted (same as in figure 1(d)). The radial distribution functions shown in figure 3(b) exhibits that the Ag–Pd cluster melted

between 600 and 800 ps, where there was a sudden temperature drop as shown in figure 3(a).

It is notable that the structural transformation in the solid state was accompanied by the gradual temperature increase before it melted. It suggests that not only the released kinetic energy after collision but also the excess surface energy released as a result of solid state transformation contributed to the temperature change of the cluster. The final temperature was proportional to the initial velocity as seen in figures 2(d) and (e), and the time gap between collision and temperature drop in melting was shortened as the initial velocity increased.

When the initial velocity was higher than 560 m s^{-1} (600 m s^{-1} in figure 1(f)), the temperature increased rapidly and it was equilibrated from an early stage as seen in figure 2(f). Because the energy was supplied sufficiently, the cluster changed to a liquid state right after collision and maintained its configuration throughout (see figure 1(f)). The final temperature was also proportional to the initial velocity.

Figure 4 shows the variation of the final temperature of the cluster with the total energy per atom. The initial velocity is also marked. The final temperature, which was averaged during the last 200 ps of each MD simulation, increased monotonically at low velocity. After the initial velocity exceeded 440 m s^{-1} (at about 850 K), the slope was lowered and a sudden temperature drop was attained at 496 m s^{-1} (at about 900 K). The Pd atoms were found to aggregate on the cluster surface after the initial velocity exceeded 440 m s^{-1} and the surface melting took place. This phenomenon infers that the melting started at around 850 K. As the released energy was absorbed as the latent heat of the structural change, the slope of the caloric curve started to flatten [31]. In order to define the surface melting point where the surface atoms start to disorder, we observed the change of the slope in figure 4 and found a pivot point from which the linearity of the initial slope started to deviate. This point was defined as the surface melting temperature in this study.

At a velocity higher than 496 m s^{-1}, the Ag and Pd atoms were eventually mixed without order and the cluster melted (see figure 3(a)). The step-type temperature drop before complete melting is similar to the results of Schebarchov and Hendy [19]. They investigated the solid–liquid coexistence and structural transition in the decahedron system of unary 887 Pd atoms by using the embedded atom potential and constructing
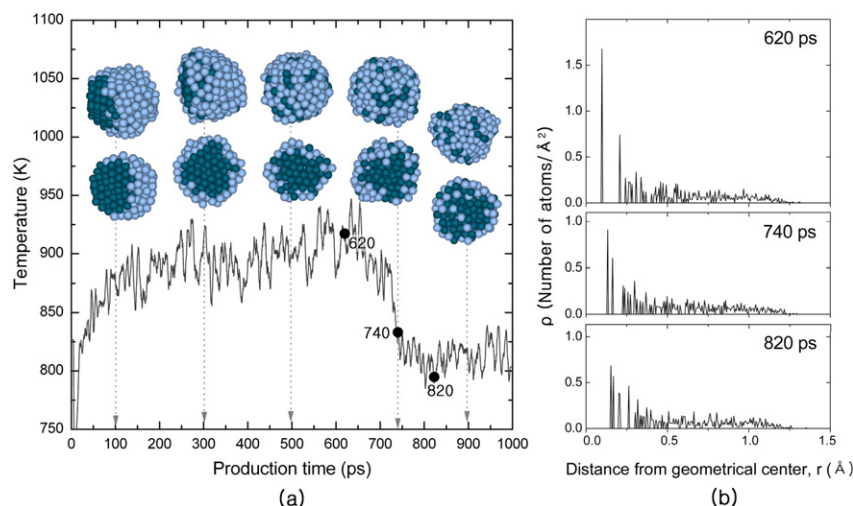
Figure 3. Evolution of atomistic configuration during collision at 500 m s^{-1}: (a) overall cluster morphology (first upper row) and cross section (second upper row) of the Ag–Pd cluster at different stages during MD simulation together with temperature changes. The Ag atoms are represented in light, the Pd atoms in dark. (b) Radial distribution functions at indicated time steps.
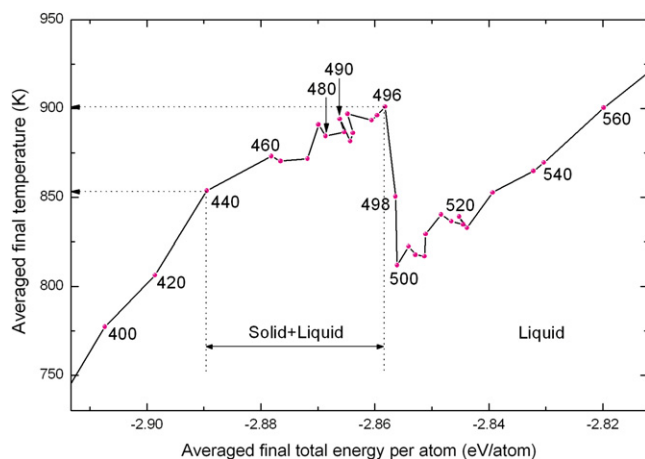

Figure 4. Variation of average final temperatures versus total energy per atom. The initial velocity is also given. The final temperature was averaged during the last 200 ps of the MD simulation.
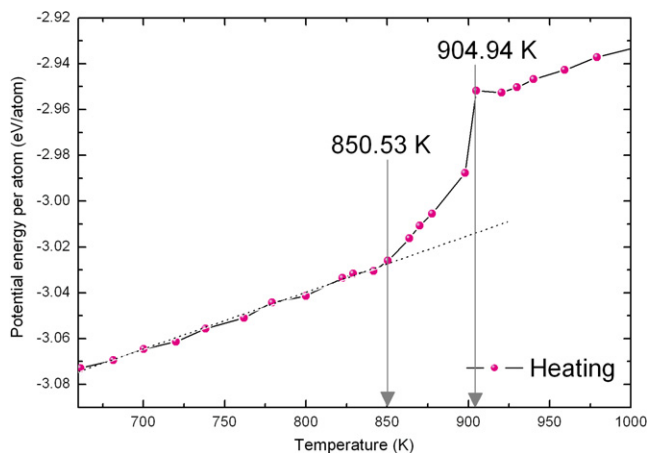

Figure 5. Variation of potential energy versus temperature according to the simulated annealing method. The cluster was heated at a rate of 3.33×10^{10} K s^{-1} but a low rate of 1.67×10^{10} K s^{-1} was applied near the melting point. The slope change of the curve indicates the melting transition of the cluster.

microcanonical (NVE) caloric curves. Their results confirmed the onset of solid–liquid coexistence at 1150 K, which is well below the bulk melting temperature of Pd, 1830 K.

After a velocity of 500 m s^{-1}, the final temperature was increased again. With regard to the surface melting of the Ag–Pd cluster, we found that the melting of the cluster starts at 850 K and that the melting is complete at temperatures above 900 K. The liquid and solid states coexist at temperatures between 850 and 900 K, which is the solid-to-liquid transition region. This region is lower than the 1290–1335 K melting range of 50Ag–50Pd (in atomic per cent) in the bulk state [32].

The collision or coalescence of two nanoclusters has been attempted as a means of investigating various structures at the solid state. In this study, however, we have used this approach as a way of observing the solid–liquid transition and of determining the melting range of bimetallic nanoclusters. We also applied the simulated annealing method to investigate

the melting behavior of this binary nanocluster and the results in figure 5 confirm that the melting of the Ag–Pd bimetallic cluster occurs between 850 and 900 K.

4. Summary

In this work, we have suggested a convenient and effective method of predicting the solid-to-liquid transition region of an Ag$_{201}$–Pd$_{201}$ bimetallic cluster. The method involves the collision of two clusters of Ag and Pd at increasing velocities.

Depending on the velocity, we can observe several different behaviors during the collision. Below 440 m s^{-1}, the final atomic configuration of the Ag–Pd cluster at 1 ns shows that two clusters were merged and mixed to form a typical core–shell structure. Between 440 and 496 m s^{-1}, the surface melting started but the inside of the cluster was still crystalline,

which confirms that the cluster was still in the solid–liquid coexistence region. In the velocity range of 496–560 m s^{-1}, the Ag–Pd cluster eventually melted. For a velocity above 560 m s^{-1}, the cluster changed to a liquid state right after the collision and maintained its configuration throughout.

With regard to the surface melting of the Ag–Pd cluster, we found that the melting starts at 850 K and is completed at 900 K. The liquid and solid states coexist between 850 and 900 K. This solid-to-liquid transition region is lower than the 1290 to 1335 K melting range of 50Ag–50Pd (in atomic per cent) in the bulk state. The additional approach of simulated annealing also confirms that the melting of the Ag–Pd bimetallic cluster occurs between 850 and 900 K.

References

[1] Barnard A S and Curtiss L A 2005 *Rev. Adv. Mater. Sci.* **10** 105
[2] Sao-Joao S, Giorgio S, Penisson J M, Chapon C, Bourgeois S and Henry C 2005 *J. Phys. Chem.* B **109** 342–7
[3] Nikolov I D 2005 *Curr. Nanosci.* **1** 211–24
[4] Wu Y, Cui Y, Huynh L, Barrelet C J, Bell D C and Lieber C M 2004 *Nano Lett.* **4** 433–6
[5] Binns C 2001 *Surf. Sci. Rep.* **44** 1–49
[6] Baletto F and Ferrando R 2005 *Rev. Mod. Phys.* **77** 371
[7] Rapallo A, Rossi G, Ferrando R, Fortunelli A, Curley B C, Lloyd L D, Tarbuck G M and Ohnston R L J 2005 *J. Chem. Phys.* **122** 194308
[8] Rossi G, Ferrando R, Rapallo A, Fortunelli A, Curley B C, Lloyd L D and Johnston R L 2005 *J. Chem. Phys.* **122** 194309
[9] Sankaranarayanan S K R S, Bhethanabotla V R and Joseph B 2005 *Phys. Rev.* B **71** 195415
[10] Cheng D J, Huang S P and Wang W C 2006 *Phys. Rev.* B **74** 064117
[11] Nam H S, Hwang N M, Yu B D and Yoon J K 2002 *Phys. Rev. Lett.* **89** 275502
[12] Shim J H, Lee B J and Cho Y W 2002 *Surf. Sci.* **512** 262–8
[13] Nam H S, Hwang N M, Yu B D, Kim D Y and Yoon J K 2005 *Phys. Rev.* B **71** 233401
[14] Lewis L J, Jensen P and Barrat J L 1997 *Phys. Rev.* B **56** 2248–57
[15] Liu H B, Jose-Yacaman M, Perez R and Ascencio J A 2003 *Appl. Phys.* A **77** 63–7
[16] Ding F, Rosén A and Bolton K 2004 *Phys. Rev.* B **70** 075416
[17] Kim H Y, Lee S H, Kim H G, Ryu J H and Lee H M 2007 *Mater. Trans.* **48** 455–9
[18] Kim H Y, Kim H G, Ryu J H and Lee H M 2007 *Phys. Rev.* B **75** 212105
[19] Schebarchov D and Hendy S C 2006 *Phys. Rev.* B **73** 121402(R)
[20] Mariscal M M, Dassie S A and Leiva E P M 2005 *J. Chem. Phys.* **123** 184505
[21] Hendy S, Brown S A and Hyslop M 2003 *Phys. Rev.* B **68** 241403(R)
[22] Sakai H 1996 *Surf. Sci.* **351** 285–91
[23] Zhao S, Wang S and Ye H 2001 *J. Phys. Soc. Japan* **70** 2953–7
[24] Cagin T, Kimura Y, Qi Y, Li H, Ikeda H, Johnson W L and Goddard W A III 1999 *Bulk Metallic Glasses* (*MRS Symp. Proc.* vol 554) ed W L Johnson *et al* (Pittsburgh, PA: Materials Research Society) pp 43–8
[25] Qi Y, Cagin T, Kimura Y and Goddard W 1999 *Phys. Rev.* B **59** 3527–33
Qi Y, Cagin T, Kimura Y and Goddard W 2002 *J. Comput.-Aided Mater. Des.* **8** 233–43
[26] Sutton A P and Chen J 1990 *Phil. Mag. Lett.* **61** 139–46
[27] Gear C W 1971 *Numerical Initial Value Problems in Ordinary Differential Equations* (Englewood Cliffs, NJ: Prentice-Hall) chapter 9
[28] Baletto F, Mottet C and Ferrando R 2003 *Phys. Rev. Lett.* **90** 135504
Baletto F, Mottet C and Ferrando R 2002 *Phys. Rev.* B **66** 155420
[29] Mottet C, Rossi G, Baletto F and Ferrando R 2005 *Phys. Rev. Lett.* **95** 35501
[30] Ruban A V, Skriver H L and Norskov J K 1999 *Phys. Rev.* B **59** 15990
[31] Schebarchov D and Hendy S C 2005 *J. Chem. Phys.* **123** 104701
[32] Karakaya I and Thompson W T 1988 *Bull. Alloy Phase Diagrams* **9** 237